

Coupled force-balance and scattering equations for nonlinear transport in quantum wires

Danhong Huang

Air Force Research Laboratory, Space Vehicles Directorate, Kirtland Air Force Base, New Mexico 87117, USA

Godfrey Gumbs

*Department of Physics and Astronomy, Hunter College of City University of New York,**695 Park Avenue, New York, New York 10065, USA*

(Received 13 April 2009; published 28 July 2009)

The coupled force-balance and scattering equations have been derived and applied to study nonlinear transport of electrons subjected to a strong dc electric field in an elastic-scattering-limited quantum wire. Numerical results have demonstrated both field-induced heating-up and cooling-down behaviors in the non-equilibrium part of the total electron-distribution function by varying the impurity density or the width of the quantum wire. The obtained asymmetric distribution function in momentum space invalidates the application of the energy-balance equation to our quantum-wire system in the center-of-mass frame. The experimentally observed suppression of mobility by a driving field for the center-of-mass motion in the quantum-wire system has been reproduced [see K. Tsubaki *et al.*, *Electr. Lett.* **24**, 1267 (1988); M. Hauser *et al.*, *Sci. Technol.* **9**, 951 (1994)]. In addition, the thermal enhancement of mobility in the elastic-scattering-limited system has been demonstrated, in accordance with a similar prediction made for graphene nanoribbons [see T. Fang *et al.*, *Phys. Rev. B* **78**, 205403 (2008)]. This thermal enhancement has been found to play a more and more significant role with higher lattice temperature and becomes stronger for a low-driving field.

DOI: [10.1103/PhysRevB.80.033411](https://doi.org/10.1103/PhysRevB.80.033411)

PACS number(s): 73.63.Nm

The force-balance equation was proposed several years ago in an effort to capture the principal physics of center-of-mass motion. This has been accomplished by introducing ensemble-averaged frictional forces based on a perturbation approximation to the carrier-distribution function. These forces are due to scattering from both impurities and phonons (at high temperatures) and contribute as one of the source terms to a Newton-type equation of motion.¹ This simple and intuitive approach was later generalized in conjunction with an energy-balance equation that includes the effect due to heating in the carrier-distribution function.² However, the employed ansatz with a quasiequilibrium carrier distribution at a different carrier temperature than a lattice temperature is expected to hold only for systems with a dominant Coulomb-pair scattering of carriers at low temperatures and high electron densities at the same time.^{3,4}

In this report, we derive coupled force-balance and scattering equations which incorporate relatively slow center-of-mass drift motion of electrons in the presence of a dc electric field as well as an ultrafast relative scattering motion of electrons. Our formalism is based on previously developed diagrammatic descriptions⁵ for momentum dissipation and for microscopic electron scattering-in and scattering-out rates. However, a previous study³ was limited only to the expanded Fokker-Planck equation for the distribution function. The center-of-mass drift velocity of electrons can be solely determined by the force-balance equation while the nonequilibrium distribution function of electrons is decided by the microscopic scattering equation with a Doppler shift⁵ but without a Boltzmann drift term,⁶ instead of by a limited-use energy-balance equation.² The exact solution of the Boltzmann transport equation in the laboratory frame was obtained for electrons in a quasi-one-dimensional quantum-dot superlattice in the presence of a strong dc or a strong ac electric field,⁷ in which both a short-range elastic scattering

and an inelastic scattering are treated microscopically. The proposed scattering equation without a drift term in the center-of-mass frame allows us to formally generalize the current theory to include both stimulated optical transitions and dephasing of induced optical coherence in the presence of a pump laser. Therefore, it establishes a direct connection between the semiclassical force-balance equation¹ and the quantum semiconductor Bloch equations.⁸⁻¹⁰ As a first step, we would like to apply our theory to the nonlinear transport of electrons under a strong dc electric field in a quantum wire by including a more realistic screened long-range electron-impurity scattering¹¹ at low temperatures and electron densities as well as at relatively high impurity densities for high-mobility samples.

For the relative scattering motion of electrons in the center-of-mass frame, our numerical results demonstrate both field-induced heating-up and cooling-down behaviors in the nonequilibrium part of the total distribution function of electrons within the nonlinear-transport regime for various impurity densities. For the center-of-mass motion, on the other hand, the field-dependent mobility is found to decrease with driving electric field^{12,13} for nonlinear electron transport. Moreover, the mobility increases with lattice temperature¹⁴ for the impurity-limited system considered in this report.

For the system shown in Fig. 1, the relevant many-body Hamiltonian in the y direction, \mathcal{H}_y , for N electrons in a quasi-one-dimensional n -doped quantum wire under an electric field \mathcal{F} along the y (wire) direction can be written as

$$\mathcal{H}_y = -\frac{\hbar^2}{2m^*} \sum_{j=1}^N \frac{\partial^2}{\partial y_j^2} - e\mathcal{F} \sum_{j=1}^N y_j + \mathcal{H}_{e-i}, \quad (1)$$

where m^* is the electron effective mass in host materials and y_j is the coordinate of the j th electron along the wire direc-

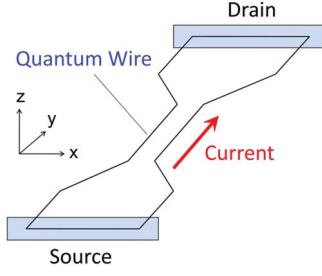


FIG. 1. (Color online) Setup for a quasi-one-dimensional quantum-wire driven by an electric field along the y (wire) direction, where the transverse confinements in the z and x directions are determined by a square quantum well and a parabolic potential, respectively. The current flowing through the quantum wire between the source and drain electrodes is indicated by a thick (red) arrow.

tion. In Eq. (1), \mathcal{H}_{e-i} represents the electron-impurity interaction and the electron-phonon interaction is neglected. In our model, we can express the center-of-mass position and momentum operators along the y direction as

$$Y_c = \frac{1}{N} \sum_{j=1}^N y_j, \quad \hat{P}_c = \sum_{j=1}^N \hat{p}_j, \quad (2)$$

where $\hat{p}_j = -i\hbar \partial / \partial y_j$ is the quantum-mechanical momentum operator of the j th electron. For simplicity, we assume that the transverse quantum confinements in both the z and x directions are so strong that only the ground states in these two directions are occupied. Therefore, we consider only the lowest single subband for the quantum wire under \mathcal{F} , at low electron densities n_0 , low lattice temperatures T , and relatively high impurity densities n_i with a thermal contact to an external heat bath, where both the electron-phonon and the Coulomb-pair scatterings of electrons in the system can be neglected.

Using the Hamiltonian in Eq. (1), Y_c , and \hat{P}_c defined in Eq. (2), we are able to calculate the center-of-mass velocity operator \hat{V}_c by means of the Heisenberg equation

$$\hat{V}_c = \frac{dY_c}{dt} = \frac{1}{i\hbar} [Y_c, \mathcal{H}_y] = \frac{1}{Ni\hbar} \sum_{j=1}^N [y_j, \mathcal{H}_y] = \frac{\hat{P}_c}{Nm^*}, \quad (3)$$

where the notation $[\hat{A}, \hat{B}] \equiv \hat{A}\hat{B} - \hat{B}\hat{A}$ for a pair of operators. Consequently, we obtain the drift velocity $v_d = \langle \hat{V}_c \rangle_{av}$ of electrons through the quasi-one-dimensional quantum wire, where $\langle \hat{A} \rangle_{av}$ represents the quantum-statistical average of an operator \hat{A} . Furthermore, we obtain from Eq. (3) the force-balance equation (similar to the Newton's equation in classical mechanics) to determine the dynamics of v_d

$$\begin{aligned} \frac{dv_d}{dt} &= \left\langle \frac{d\hat{V}_c}{dt} \right\rangle_{av} = \frac{1}{Nm^*i\hbar} \left\langle \sum_{j=1}^N [\hat{p}_j, \mathcal{H}_y] \right\rangle_{av} \\ &= \frac{e\mathcal{F}}{m^*} + \mathcal{A}_i\{[f], v_d\}, \end{aligned} \quad (4)$$

where the $\mathcal{A}_i\{[f], v_d\}$, which is a functional of $[f_k]$ and f_k represents the total nonequilibrium distribution of k -state electrons in relative scattering motions, is the ensemble-averaged resistive acceleration (related to an impurity frictional force) due to scattering of electrons by impurities, and the resistive acceleration due to electron-phonon scattering is neglected. In addition, $\mathcal{A}_i\{[f], v_d\}$ in Eq. (4) is given by^{3,5}

$$\begin{aligned} \mathcal{A}_i\{[f], v_d\} &= \left(\frac{N_i}{N} \right) \frac{2\pi}{\hbar} \sum_{k,k'} |U_i(|k' - k|)|^2 [v(k') - v(k)] (f_k - f_{k'}) \\ &\quad \times \delta[\varepsilon(k') - \varepsilon(k) + \hbar(k' - k)v_d]. \end{aligned} \quad (5)$$

In Eq. (5), $v(k) = \hbar^{-1} d\varepsilon(k)/dk = \hbar k/m^*$ is the group velocity, $\varepsilon(k) = \hbar^2 k^2/2m^*$ is the kinetic energy of electrons, k is the wave number in the y direction, $N = 2\sum_k f_k$ is the total number of electrons, N_i is the number of ionized donors in the system, and the last term containing v_d is for the Doppler shift.^{3,5} The explicit expression for $|U_i(|q|)|^2$ in Eq. (5) is presented below in Eq. (8).

By assuming a Boltzmann-type collision term⁶ for electron-impurity scattering, the microscopic scattering equation for relative motion of electrons in the center-of-mass frame can be expressed as^{3,5}

$$\begin{aligned} \frac{dg(k)}{dt} &= \mathcal{W}_k^{(in)}\{[f], v_d\} (1 - f_k) - \mathcal{W}_k^{(out)}\{[f], v_d\} f_k \\ &= \mathcal{W}_k^{(in)}\{[f], v_d\} [1 - f_k^{(0)} - g(k)] \\ &\quad - \mathcal{W}_k^{(out)}\{[f], v_d\} [f_k^{(0)} + g(k)], \end{aligned} \quad (6)$$

where $f_k = f_k^{(0)} + g(k)$, $f_k^{(0)} = 1 / \{\exp\{[\varepsilon(k) - \mu_0]/k_B T\} + 1\}$ is the Fermi function for thermal-equilibrium electrons, μ_0 is the chemical potential, $g(k)$ represents the nonequilibrium part of the total electron-distribution function, and $\sum_k g(k) \equiv 0$ ensures the conservation of the total number of electrons in the system.¹⁵ The quantities $\mathcal{W}_k^{(in)}\{[f], v_d\}$ and $\mathcal{W}_k^{(out)}\{[f], v_d\}$ in Eq. (6) are the scattering-in rate for electrons in the final k state and the scattering-out rate for electrons in the initial k state.

For the relative electron-impurity scattering in Eq. (6), we have^{3,5}

$$\begin{aligned} &\begin{bmatrix} \mathcal{W}_k^{(in)}\{[f], v_d\} \\ \mathcal{W}_k^{(out)}\{[f], v_d\} \end{bmatrix} \\ &= N_i \frac{4\pi}{\hbar} \sum_{k'}^{(k' \neq k)} |U_i(|k - k'|)|^2 \\ &\quad \times \begin{bmatrix} f_{k'} \delta[\varepsilon(k) - \varepsilon(k') + \hbar(k - k')v_d] \\ (1 - f_{k'}) \delta[\varepsilon(k') - \varepsilon(k) + \hbar(k' - k)v_d] \end{bmatrix}, \end{aligned} \quad (7)$$

where the electron-phonon scattering is neglected and the screened long-range Coulomb interaction between electrons and ionized impurity atoms is given by

$$|U_i(|q|)|^2 = \left[\frac{Z^* e^2}{2\pi\epsilon_0\epsilon_r L\epsilon(q)} \right]^2 \left[\int_0^{+\infty} d\eta \exp\left(-\frac{\eta^2 \ell^2}{4}\right) \times \frac{\mathcal{R}(\eta, q, z_0)}{\sqrt{\eta^2 + q^2}} \right]^2. \quad (8)$$

Here, Z^* is the charge number of impurity atoms, L is the length of a quantum wire, ϵ_r is the dielectric constant of the host material, and 2ℓ measures the width of the spatial distribution of the ground-state wave function in the transverse x direction. The form factor in Eq. (8) for the quantum-well confinement is calculated as¹¹

$$\mathcal{R}(\eta, q, z_0) = \int_{-\infty}^{+\infty} dz |\xi_0(z)|^2 \exp(-\sqrt{\eta^2 + q^2}|z - z_0|), \quad (9)$$

where $\xi_0(z)$ is the ground-state wave function of the square quantum well in the z direction and z_0 is the position of a single δ -doping layer inside the quantum well. The static dielectric function $\epsilon(q)$ employed in Eq. (8) is given by

$$\begin{aligned} \epsilon(q) = 1 + & \left(\frac{e^2}{\pi^2 \epsilon_0 \epsilon_r \hbar v_F} \right) \int_{-\infty}^{\infty} dx \int_{-\infty}^{\infty} dx' \left(\frac{1}{\pi \ell^2} \right) \\ & \times \exp\left(-\frac{x^2 + x'^2}{\ell^2}\right) \int_{-\infty}^{\infty} dz \int_{-\infty}^{\infty} dz' |\xi_0(z)|^2 \\ & \times K_0(|q| \sqrt{(x-x')^2 + (z-z')^2}) |\xi_0(z')|^2, \quad (10) \end{aligned}$$

where $v_F = \hbar k_F / m^*$ is the Fermi velocity, $k_F = \pi n_0 / 2$ is the Fermi wave number, $n_0 = N/L$ is the linear electron density, and $K_0(x)$ is the modified Bessel function of the second kind. The quantum-well wave function $\xi_0(z)$ in Eqs. (9) and (10) is calculated by using the self-consistent Hartree-Fock approximation.¹⁶

In our numerical calculations, we have chosen the following parameters for the quantum wire: $m^* = 0.067 m_0$ (m_0 is the free-electron mass), appropriate for GaAs, $\ell = 37.5 \text{ \AA}$, $n_0 = 5 \times 10^5 \text{ cm}^{-1}$, $n_i/n_0 = 0.01$ ($n_i = N_i/L$), $Z^* = 1$, $T = 5 \text{ K}$, and $\epsilon_r = 12$. For the square quantum well in the z direction, we choose the well width $L_W = 75 \text{ \AA}$, the barrier height $V_0 = 280 \text{ meV}$, the δ -doping-layer position $z_0 = 0$, the well effective mass $m_W = 0.067 m_0$, and barrier effective mass $m_B = 0.073 m_0$. From these parameters, we calculate the Fermi velocity $v_F = 13.6 \times 10^6 \text{ cm/s}$, the Fermi wave number $k_F = 7.854 \times 10^{-3} \text{ \AA}^{-1}$, and the chemical potential $\mu_0 = 3.22 \text{ meV}$. Whenever we use different values of the parameters in our calculations, such as T , n_i/n_0 and \mathcal{F} , this is directly indicated in the figure captions.

Figures 2(a) and 2(b) report on $g(k)$ at $T = 5 \text{ K}$ as functions of the dimensionless wave number k/k_F for a number of electric field strengths \mathcal{F} at a lower impurity density $n_i/n = 0.01$ in (a) and at a higher impurity density $n_i/n = 0.04$ in (b). At the lower impurity density in Fig. 2(a), more and more electrons are driven back from high-energy states to states of low energy as we increase the electric field over the range $\mathcal{F} = 1 - 8 \text{ V/cm}$ within the regime of nonlinear electron transport. The transition from linear transport, where Ohm's law is applicable, to nonlinear transport can be attributed to the field-enhanced term $\mathcal{A}_i\{[f], v_d\}$ in Eq. (5), which

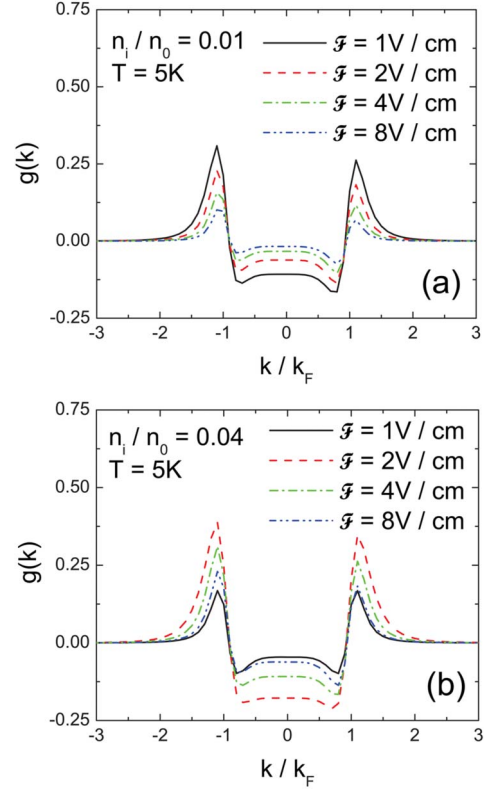


FIG. 2. (Color online) Calculated nonequilibrium contributions $g(k)$ with $T = 5 \text{ K}$ as functions of k/k_F for four chosen values of dc electric field, i.e., $\mathcal{F} = 1$ [solid (black) curves], 2 [dashed (red) curves], 4 [dash-dotted (green) curves], and 8 V/cm [dash-dot-dotted (blue) curves]. In (a), we set $n_i/n_0 = 0.01$ while we have $n_i/n_0 = 0.04$ in (b).

increases much faster than the linear driving term in Eq. (4) at high \mathcal{F} . A large Doppler-shift term in Eq. (7) assists the scattering of electrons out from high-energy states to low-energy states, leading to a cooling down of electrons. However, when the impurity density is increased to $n_i/n = 0.04$ in Fig. 2(b), electrons are first heated up when \mathcal{F} changes from 1 to 2 V/cm. This is closely followed by a cooling down of electrons as \mathcal{F} is further increased from 2 all the way up to 8 V/cm. Therefore, a stronger electric field \mathcal{F} is required for initiating an electronic cooling-down process in a system with a higher impurity density. Since the reduction in quantum-wire width ℓ is equivalent to a higher impurity density, as shown in Eqs. (7) and (8), we expect that the same argument can also apply to the wire width (not shown).

Plots for the nonequilibrium part of the total electron-distribution function in Fig. 2 exhibit both electron cooling-down and heating-up behaviors when different driving fields \mathcal{F} and impurity densities n_i are used. This is a demonstration of the effects of the relative scattering motion of electrons with impurities in the center-of-mass frame. The other important feature of impurity scattering is manifested in the ensemble-averaged frictional force term $\mathcal{A}_i\{[f], v_d\}$ in Eq. (4), which directly leads to a nonlinear dependence of the drift velocity v_d as a function of the driving electric field \mathcal{F} in the high-field transport regime. The nonlinear \mathcal{F} dependence for the drift velocity v_d in (a), as well as for the de-

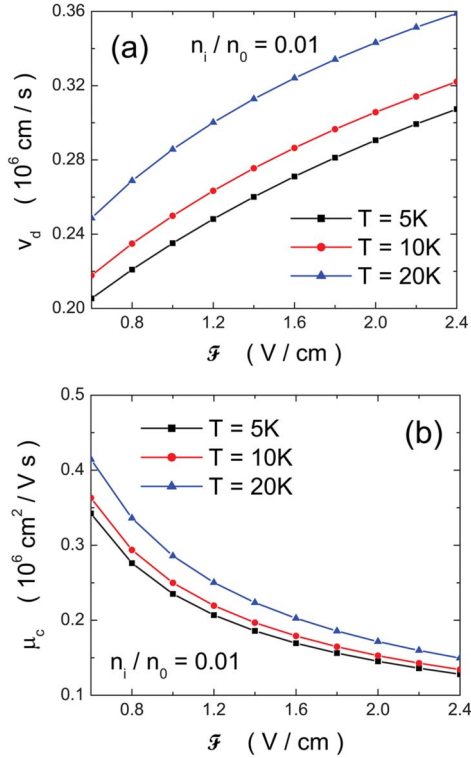


FIG. 3. (Color online) Plots of (a) the drift velocity v_d and (b) the mobility $\mu_c = v_d/\mathcal{F}$ with $n_i/n_0 = 0.01$ as functions of \mathcal{F} for three chosen values of temperature T : $T = 5$ K (solid squares on black curves), 10 K (solid circles on red curves), and 20 K (solid triangles on blue curves).

duced mobility $\mu_c = v_d/\mathcal{F}$ in (b), are shown in Fig. 3 with $n_i/n_0 = 0.01$ and three lattice temperatures. For any chosen value of \mathcal{F} in Fig. 3(a), v_d increases with T , and this thermal enhancement becomes more significant for higher T . Similar thermal enhancement in mobility was also obtained in semiconducting graphene nanoribbons for elastic scattering.¹⁴ Furthermore, we find from Fig. 3(b) that μ_c decreases with \mathcal{F} for each fixed value of T . This field-induced mobility suppression at low T was experimentally observed in quantum-

wire systems.^{12,13} In addition, the thermal enhancement in μ_c becomes stronger at low values of \mathcal{F} .

Two large positive peaks around $k/k_F = \pm 1$ at a low T were found to be nonsymmetrical with respect to $k=0$ in the nonequilibrium part $g(k)$ of the total distribution function. This is in contradiction with the ansatz for introducing the energy-balance equation. Electrons were found to be heated up first by a moderate \mathcal{F} at low n_i but they become cooled down when n_i is increased. This thermal-switching behavior is a consequence of the dynamical balance between electron scattering-in and scattering-out processes for the relative motion of electrons in the center-of-mass frame. Moreover, a larger threshold dc electric field is required for starting up the electron cooling-down process, i.e., electrons are driven back from high-energy states to low-energy ones as we increase \mathcal{F} within the nonlinear-transport regime, in the system with a higher n_i (or with a smaller quantum-wire width ℓ). We chose a value of $n_i/n_0 = 0.01$ since it is reasonable to assume that the ionized-impurity density is less than the electron density. Our results are not changed qualitatively for other low values of impurity density and this chosen value should allow us to arrive at reasonable conclusions concerning transport. For chosen \mathcal{F} , v_d increases with T . This thermal enhancement has been found to become more and more significant as T was increased. Although the calculated v_d is less than $v_F = 1.36 \times 10^7$ cm/s for the range of values of \mathcal{F} , we believe that v_d could be made even larger at increased \mathcal{F} and T . In addition, the thermal enhancement of μ_c becomes stronger for a low \mathcal{F} . Our calculations have shown that μ_c is roughly proportional to $1/n_i$ when \mathcal{F} is fixed and it increases with T almost at a uniform rate independent of n_i and \mathcal{F} . The introduced microscopic scattering equation without the Boltzmann drift term in the center-of-mass frame allows us establishing the connection between the force-balance equation for transport and the semiconductor Bloch equations for optical transitions.

D.H. would like to thank the Air Force Office of Scientific Research (AFOSR) for its support. G.G. was supported by Contract No. FA 9453-07-C-0207 of AFRL.

¹C. S. Ting, S. C. Ying, and J. J. Quinn, Phys. Rev. B **14**, 4439 (1976).

²X. L. Lei and C. S. Ting, Phys. Rev. B **32**, 1112 (1985).

³D. H. Huang, T. Apostolova, P. M. Alsing, and D. A. Cardimona, Phys. Rev. B **69**, 075214 (2004).

⁴X. L. Lei, Phys. Rev. B **77**, 033203 (2008).

⁵D. H. Huang, P. M. Alsing, T. Apostolova, and D. A. Cardimona, Phys. Rev. B **71**, 195205 (2005).

⁶J. M. Ziman, *Principles of the Theory of Solids*, 2nd ed. (Cambridge Press, Cambridge, 1972), pp. 212–215.

⁷D. H. Huang, S. K. Lyo, and G. Gumbs, Phys. Rev. B **79**, 155308 (2009).

⁸M. Lindberg and S. W. Koch, Phys. Rev. B **38**, 3342 (1988).

⁹F. Rossi and T. Kuhn, Rev. Mod. Phys. **74**, 895 (2002).

¹⁰M. Kira and S. W. Koch, Prog. Quantum Electron. **30**, 155 (2006).

¹¹X. L. Lei, J. L. Birman, and C. S. Ting, J. Appl. Phys. **58**, 2270 (1985).

¹²M. Hauser, E. Gornik, C. Winer, M. Baur, G. Böhm, and G. Weimann, Semicond. Sci. Technol. **9**, 951 (1994).

¹³K. Tsubaki, T. Fukui, Y. Tokura, H. Saito, and N. Susa, Electron. Lett. **24**, 1267 (1988).

¹⁴T. Fang, A. Konar, H. Xing, and D. Jena, Phys. Rev. B **78**, 205403 (2008).

¹⁵S. K. Lyo and D. H. Huang, Phys. Rev. B **64**, 115320 (2001).

¹⁶D. H. Huang and M. O. Manasreh, Phys. Rev. B **54**, 5620 (1996).